International Journal of Microwave and Wireless Technologies

cambridge.org/mrf

An optimal circular antenna array design considering the mutual coupling employing ant lion optimization

Avishek Das[1], Durbadal Mandal[2] and Rajib Kar[2]

[1]Department of Electronics and Communication Engineering, HIT, Haldia, 721657, India and [2]Department of Electronics and Communication Engineering, NIT, Durgapur, 713209, India

Research Paper

Cite this article: Das A, Mandal D, Kar R (2021). An optimal circular antenna array design considering the mutual coupling employing ant lion optimization. *International Journal of Microwave and Wireless Technologies* **13**, 164–172. https://doi.org/10.1017/S1759078720000914

Received: 3 December 2019
Revised: 14 June 2020
Accepted: 15 June 2020
First published online: 9 July 2020

Key words:
3-dB beam width; ant lion optimization; circular antenna array; mutual coupling; side lobe level

Author for correspondence:
Avishek Das,
E-mail: avishek.uit0408@gmail.com

Abstract

This paper presents an efficient approach for the design of a non-uniform single ring circular antenna array (CAA) for the synthesis of the optimal far-field radiation pattern. A recently proposed meta-heuristic-based optimization technique known as ant lion optimization (ALO) is applied in this paper to determine the optimum set of current amplitude excitation weights and the inter-element distance among the array elements to reduce the side lobe level (SLL) and 3-dB beam width considering the mutual coupling effect. The results achieved by employing the ALO algorithm are compared with the uniform radiation pattern and with those of the recently reported literature containing equal sets of elements to prove the superiority of ALO algorithm. Three different design examples of 8, 10, and 12 elements CAA are presented, and their performances are compared to illustrate the capability of the ALO algorithm-based approach over those of the recently reported literature.

Introduction

A proficient antenna array design has a remarkable role in the wireless communication system. A number of research works on the antenna array design are going on over the last few decades for the improvement of far-field radiation characteristics. The growing number of traffic in radio frequency (RF) spectrum has compelled the antenna design engineers to realize the antenna array having low side lobe level (SLL) as well as narrow 3-dB beam width. The narrow beam width is necessary to achieve the high directivity, whereas, a low SLL is the utmost design criteria to minimize the interference with the other radiating systems driving in the same frequency band [1, 2]. However, the antenna array design with low SLL as well as narrow 3-dB beam width is a challenging one because the improvement of one design aspect will deteriorate the other [1, 2] and hence, both the design criteria will never be met at the same time.

The presence of mutual coupling between the array elements degrades the performance of the antenna array design [3, 4]. But a very few attempts have been made in the past to reduce the effect of mutual coupling [5, 6] among the array elements. In this paper, the authors have applied an efficient method [5] for the CAA design to reduce the mutual coupling among the elements of the array. The reciprocal of driving impedance is called driving admittance which is also known as mutual coupling among the array elements [2]. The performance of the transmission and reception of the RF signal for the synthesis of CAA is heavily affected due to the mutual coupling [3]. This paper presents method [5] for minimizing the mutual coupling among the elements of the array by proper controlling the feed currents excitation which in turn reduces the driving admittance of each identical element of the array. The summation of driving admittance of all the elements of the array is reduced efficiently to minimize the mutual coupling among the elements of the array by optimizing the current amplitude excitation weights using different optimization techniques. The approach presented here is a generic one and can be applied for the radiation pattern synthesis of circular antenna array with any number of array elements.

The main objective of this paper is to design a circular antenna array with a low SLL as well as a narrow 3-dB beam width in the presence of mutual coupling. These two prime design criteria of CAA are obtained by the optimal current amplitude excitation weights and the inter-element distance among the elements of the array while the phase difference between any two elements is kept at zero. The method of null control in the far-field radiation pattern using evolutionary optimization technique is discussed in [7]. The numerical results show the comparison among genetic algorithm (GA) [8–10], particle swarm optimization (PSO) [11–13], simulated annealing (SA) [14, 15], biogeography-based optimization (BBO) [16], firefly algorithm (FFA) [17], moth flame optimization (MFO) [18], and ALO [19–22] algorithm-based approaches for the design of CAA. Panduro *et al.* in [10], employed GA for SLL reduction of 8, 10, and 12 elements non-uniform CAA design. PSO is applied in [13] for the design of non-uniform CAA of 8, 10, and 12 elements. Rattan *et al.* in [15], have applied SA for the

© Cambridge University Press and the European Microwave Association 2020

CAMBRIDGE UNIVERSITY PRESS

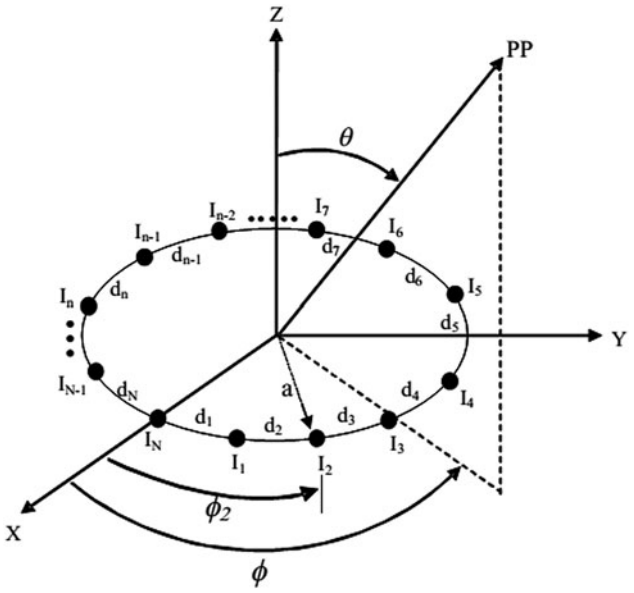


Fig. 1. The geometry of *N*-elements CAA in the *x*–*y* plane.

optimization of 8, 10, and 12 elements CAA of isotropic radiators. BBO is applied in [16] for the synthesis of 8, 10, and 12 elements CAA. Sharaqa *et al.* in [17], applied FFA for the synthesis of the same CAA. Morabito *et al.* in [18], proposed a simple method based on the aperture antenna theory to give a more complete and assorted overview of the recent developments for the orbital angular momentum (OAM) antennas. In [23], Das *et al.* have employed MFO optimization technique for the synthesis of the linear antenna array (LAA) and CAA. However, the method discussed in [23] is not practically suitable because the mutual coupling effect is not considered there for design purpose. But, the effect of mutual coupling is an indispensable part for all practical antenna array design issue. In this paper, the authors propose the controlling method of the current ratio for mutual coupling compensation using evolutionary optimization techniques for the design of CAA structure of 8, 10, and 12 elements and the results obtained by employing ALO algorithm are compared with the state-of-the-art algorithm.

The rest part of the paper is arranged as follows: Section II presents the design equation of CAA. Section III shows a brief discussion of the applied algorithm for the design of CAA. Comparative simulation results are presented in Section IV. Finally, Section V concludes the paper.

Design equation

Figure 1 shows an *N* elements CAA in the *x*–*y* plane having a radius "*a*" and scanning a point *PP* in the far-field. The radiation pattern of the CAA is represented by its array factor (*AF*), as all the elements of the array are isotropic, and it is given in (1) [1].

$$AF = \sum_{n=1}^{N} I_n \exp\left(j[ka \sin\theta \cos(\varphi - \varphi_n) + \alpha_n]\right), \quad (1)$$

where

$$ka = \frac{2\pi a}{\lambda} = \sum_{i=1}^{N} d_i, \quad (2)$$

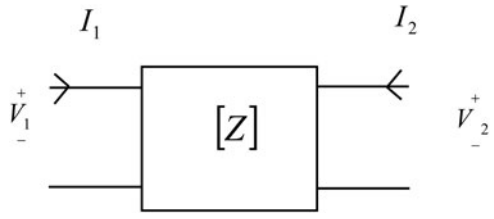


Fig. 2. Two-port network.

$$\varphi_n = \left(\frac{2\pi}{ka}\right) \sum_{i=1}^{n} d_i, \quad (3)$$

$k = 2\pi/\lambda$, λ is the wavelength of operation, θ and φ represent the elevation and azimuth angle, respectively.φ_n represents the angular position of the *n*th element in the *x*–*y* plane.

The array factor (*AF*) is assumed to be in the *x*–*y* plane, as presented in this paper. Thus the following changes are made.

$$\theta = \frac{\pi}{2}, \quad \alpha_n = -ka\cos(\varphi_0 - \varphi_n). \quad (4)$$

Thus, the *AF* can be rewritten as

$$AF = \sum_{n=1}^{N} I_n \exp\left(jka[\cos(\varphi - \varphi_n) - \cos(\varphi_0 - \varphi_n)]\right), \quad (5)$$

where I_n is the current excitation amplitude weight of the n^{th} element of the array, d_n is the inter-element spacing between the elements "*n*" and "$n+1$".φ_0 is the direction of the main beam, which is chosen to be zero.

The design goal of this paper is to determine the optimal current excitation amplitude weights and inter-element distance for the synthesis of far-field radiation pattern having low SLL as well as narrow 3-dB beam width considering the mutual coupling effect.

In an antenna array, the presence of other antenna elements alters the current distribution, the electromagnetic field distribution and in turn, the input impedance of all the elements of the array. So, the performance of an individual antenna in an array depends not only on its feed currents but also on the currents of its neighbor elements. The input impedance of an antenna in the presence of other array elements is called the driving impedance, which depends on the current ratio, the self-impedance, and the mutual impedance. It is also observed by using induced EMF method [1] that these three parameters are not related to each other; hence, change in the value of any one of the parameters will change the driving impedance value, keeping the other two parameter values unaltered.

Now, to illustrate the method, consider an antenna array which consists of two elements. So, the antenna array system can be represented by a two-port network, as shown in Fig. 2.

$$V_1 = Z_{11}I_1 + Z_{12}I_2, \quad (6)$$

$$V_2 = Z_{21}I_1 + Z_{22}I_2, \quad (7)$$

where Z_{11} and Z_{22} are the self-impedances of antenna 1 and antenna 2, respectively. Z_{12} and Z_{21} are the mutual impedances due to the current at port 2 and port 1, respectively.

https://doi.org/10.1017/S1759078720000914 Published online by Cambridge University Press

The presence of other elements will modify the input impedance values and are represented by (8) and (9).

$$Z_{1d} = \frac{V_1}{I_1} = Z_{11} + Z_{12}\left(\frac{I_2}{I_1}\right), \tag{8}$$

$$Z_{2d} = \frac{V_2}{I_2} = Z_{22} + Z_{21}\left(\frac{I_1}{I_2}\right), \tag{9}$$

where Z_{1d} and Z_{2d} represent the driving impedance of antenna 1 and antenna 2, respectively, which depend on three independent parameters, namely, the current ratio (I_1/I_2), the self-impedance, and the mutual impedance value.

The analysis of driving impedance using the induced EMF method [1] shows that even though the driving impedance of each array element depends upon the above three parameters, these parameters do not depend on each other.

The induced EMF method [1] is employed to derive the driving impedance of a non-uniform CAA of N elements. The analysis and understanding of the mutual coupling between the elements of an array can be considerably simplified by considering a non-uniform CAA of N elements which can be represented by an n-port network. The voltage–current relationship in an n-port network is given in (10).

$$[V_n] = [Z_n][I_n], \tag{10}$$

$$\begin{bmatrix} V_1 \\ V_2 \\ \vdots \\ V_n \end{bmatrix} = \begin{bmatrix} Z_{11} & Z_{12} & \cdots & Z_{1n} \\ Z_{21} & Z_{22} & \cdots & Z_{2n} \\ \vdots & \vdots & \vdots & \vdots \\ Z_{n1} & Z_{n2} & \cdots & Z_{nn} \end{bmatrix} \begin{bmatrix} I_1 \\ I_2 \\ \vdots \\ I_n \end{bmatrix}, \tag{11}$$

$$\begin{aligned} V_1 &= Z_{11}I_1 + Z_{12}I_2 + \cdots + Z_{1n}I_n \\ V_2 &= Z_{21}I_1 + Z_{22}I_2 + \cdots + Z_{2n}I_n \\ &\vdots \\ V_n &= Z_{n1}I_1 + Z_{n2}I_2 + \cdots + Z_{nn}I_n \end{aligned}. \tag{12}$$

So, the driving impedance can be represented as

$$\begin{aligned} Z_{1d} &= \frac{V_1}{I_1} = Z_{11} + \quad Z_{12}\frac{I_2}{I_1} + \quad \cdots + \quad Z_{1n}\frac{I_n}{I_1} \\ Z_{2d} &= \frac{V_2}{I_2} = Z_{21}\frac{I_1}{I_2} + \quad Z_{22} + \quad \cdots + \quad Z_{2n}\frac{I_n}{I_2} \\ &\vdots \qquad\qquad \vdots \qquad\quad \vdots \qquad\quad \vdots \\ Z_{nd} &= \frac{V_n}{I_n} = Z_{n1}\frac{I_1}{I_n} + \quad Z_{n2}\frac{I_2}{I_n} + \quad \cdots + \quad Z_{nn} \end{aligned} Z. \tag{13}$$

The sum of all the driving impedance values for each element of the array is represented as Z_{Dmn}.

$$Z_{Dmn} = \sum_{m=1}^{n} Z_{md} = \sum_{m=1}^{n}\sum_{n=1}^{n} Z_{mn}\frac{I_n}{I_m}, \tag{14}$$

where Z_{md} is the driving impedance of the individual array elements. Z_{mn} is the mutual impedance and I_n/I_m is the current ratio. The analytical expression for the driving impedance calculation using the EMF method for a two-element linear dipole using closed-form solution [1] shows that the self and mutual impedance values are not related to the current ratio. Hence, in the proposed method, authors have minimized the reciprocal of driving impedance which is also called the driving admittance for the reduction of mutual coupling among the array elements by optimizing the current ratio keeping the Z_{mn}value unaltered.

Now to achieve the design objective, a suitable Cost Function (CF) needs to be formulated to reduce the SLL and 3-dB beam width in the presence of the mutual coupling effect as given in (15).

$$\begin{aligned} CF = &W_1 \times \frac{|AF(\theta_{ms1}, I_{n,i}) + AF(\theta_{ms2}, I_{n,i})|}{|AF(\theta_{\max}, I_{n,i})|} + W_2 \times \left(\frac{1}{Z_D}\right) \\ &+ W_3 \times [3dBBW_{Computed} - 3dBBW(I_{n,i} = 1)], \end{aligned} \tag{15}$$

where Z_D is the driving impedance of CAA due to the current ratio and is given in (16).

$$Z_D = \sum_{n=1}^{N}\left(\frac{\sum_{i=1}^{N} I_{n,i}}{I_{n,i}}\right). \tag{16}$$

Here, W_1, W_2, and W_3 are the weighting factors and $\theta_{\max}$ represents the maximum value of θ; θ_{ms1} and θ_{ms2} represent the maximum side lobe angles below and above $\theta_{\max}$; $I_{n,i}$ is the current excitation amplitude weight of $(n, i)^{th}$ element. 3-dB beam width is the angular width between the 3-dB points on both sides of the main beam. Thus, 3 $dBBW_{Computed}$ and 3 $dBBW$ ($I_{n,i} = 1$) refer to the computed 3 dB beam width for the non-uniform excitation and the uniform excitation case, respectively. The third term in equation (15) is computed only if 3 $dBBW_{Computed}$ >3 $dBBW$ ($I_{n,i} = 1$).

The first term on the right-hand side (RHS) of (15) is used for suppressing the SLL by minimizing the ratio of the summation of AF values positioned on the maximum side lobe at the angle of the upper and lower band of the radiation pattern, respectively, to the maximum AF value; the second term of (15) is used to reduce the driving admittance by optimizing the current ratio for minimizing the mutual coupling, and the third term is used to reduce the 3-dB beam width by minimizing the difference, achieved by non-uniform excitation and uniform excitation, respectively. In this paper, the far-field radiation patterns of 8, 10, and 12 elements CAA are optimized for minimizing the SLL, 3-dB beam width and mutual coupling between the elements of the array. ALO algorithm controls the current amplitude excitation weights and inter-element distances between the array elements to minimize the CF.

Ant lion optimization (ALO) algorithm

The main inspiration of the ALO algorithm is deduced from the foraging behavior of the ant lions larvae. An ant lion larva digs different sized cone-shaped pits in the sand by throwing out sands by its massive jaw. The larvae hide below the pits and waite for insects to be trapped in the pit. The edge of the cone is made very sharp for insects to slide down to the bottom of the pit easily. When the ant lion senses that a prey is in the trap, it tries to catch it. The ant lions intelligently throw sands

https://doi.org/10.1017/S1759078720000914 Published online by Cambridge University Press

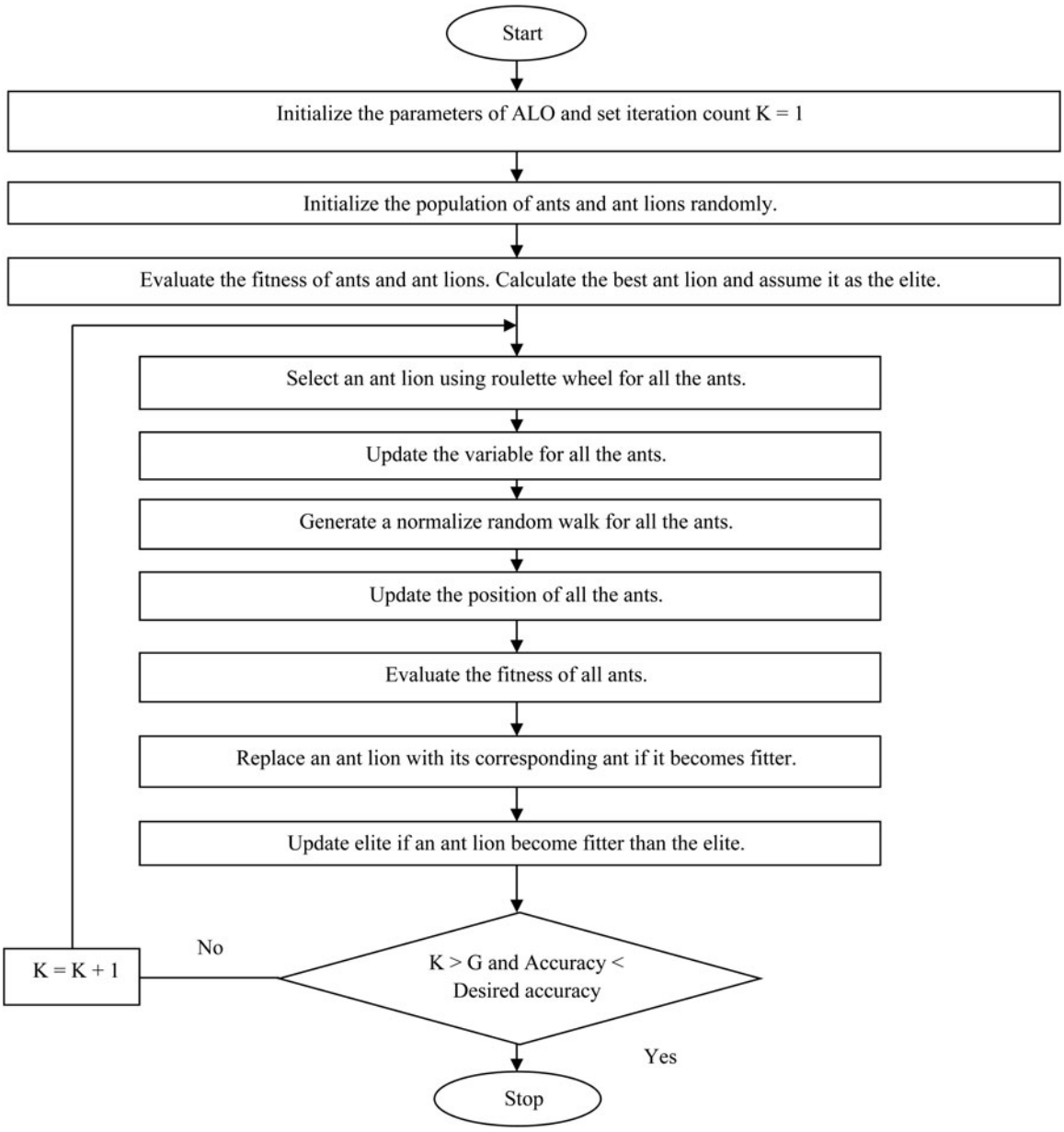


Fig. 3. Flowchart for ALO algorithm.

to the edge of the pit for the prey to slide down to the bottom of the pit, when the trapped insects try to escape from the pit. After catching the prey, the prey is pulled under the soil and consumed. The behaviors of ant lions and their prey are modelled mathematically in ALO and are discussed in details in [19–22]. The main steps of the ALO algorithm for the CAA optimization problem are given as a flowchart in Fig. 3.

Results and discussions

ALO algorithm is extensively executed to achieve the normalized optimized current amplitude excitation weights and inter-element distance of the 8, 10, 12 elements CAA. The ALO algorithm is run for 50 times with their best control parameters [24] by using MATLAB 7.5 version on Intel Core (TM) 2 processor with 3.00 GHz with 3 GB RAM to obtain the best results.

Numerical results

The results achieved by employing ALO algorithm considering the mutual coupling for CAA design is compared with the uniform pattern and with the state-of-the-art algorithms containing equal sets of the elements which do not consider the mutual coupling for CAA design.

Table 1 shows the results of the uniformly excited ($I_{n,i} = 1$) and uniformly spaced ($d = \lambda/2$) CAA of 8, 10, 12 elements and it is termed as the uniform pattern in the graphical plots in the presented work. The SLL values for the uniform pattern of 8, 10, 12 elements CAA are −4.17 dB, −3.597 dB, and −7.165 dB, respectively, whereas, the 3-dB beam widths of the arrays mentioned above are 32.32°, 25.84°, and 21.52°. The First Null Beam Width (FNBW) values of 8, 10, 12 elements CAA are 69.98°, 55.66°, and 46.22°, respectively, and the mutual coupling values are 0.0156, 0.0100, and 0.0069. The results of Table 1

https://doi.org/10.1017/S1759078720000914 Published online by Cambridge University Press

Table 1. The initial value of SLL, 3-dB beam width, and FNBW for uniformly excited ($I_{n,i} = 1$) and uniformly spaced ($d = \lambda/2$) CAA.

No. of Elements	SLL (dB)	3-dB beam width (°)	FNBW (°)	Mutual Coupling
8	−4.17	32.32	69.98	0.0156
10	−3.597	25.84	55.66	0.0100
12	−7.165	21.52	46.22	0.0069

show that 3-dB beam width and mutual coupling values of the uniform pattern for 8, 10, 12 elements CAA are reduced with the increase in the array elements for the uniform pattern synthesis of CAA.

The comparative results of GA [10], PSO [13], SA [15], BBO [16], FFA [17], MFO [23], and ALO algorithms for non-uniformly excited and non-uniformly spaced 8 elements CAA design are shown in Table 2. The table contains the normalized values of current amplitude excitation weights, inter-element spacing, SLL, 3-dB beam width, and mutual coupling values obtained by using different algorithms for 8 elements CAA design. The SLL value of uniform pattern for 8 elements CAA design is −4.17 dB and the value improves to −9.811 dB, −10.799 dB, −12.00 dB, −12.24 dB, −13.00 dB, and −15.78 dB by using GA, PSO, SA, BBO, FFA, and MFO algorithm, respectively. Now by employing ALO algorithm far better results of SLL of −15.87 dB is achieved. The reduction of SLL value is improved to 61.75%, 46.95%, 32.25%, 29.65%, 22.07%, and 0.57% with respect to GA, PSO, SA, BBO, FFA, MFO algorithm as given in Table 2. The 3-dB beam width obtained by using GA, PSO, SA, BBO, FFA, MFO, and ALO algorithms is 32°, 32°, 30.60°, 31.60°, 33.10°, 32.76°, and 30.16°, respectively, whereas, the mutual coupling values are 0.0118, 0.0080, 0.0193, 0.0203, 0.0040, 0.0149, 0.0146, respectively.

The results obtained by using different algorithms for the non-uniformly excited and non-uniformly spaced 8 elements CAA design are graphically plotted in Fig. 4. The figure shows the far-field radiation patterns obtained by using different algorithms and the comparison with the uniform pattern obtained by using uniform excitation to all the array elements having a half wavelength inter-element spacing. Figure 4 reveals that the ALO algorithm yields the lowest SLL value and lowest 3-dB beam width as compared to other well-established algorithms. The figure shows the superiority of the ALO algorithm over other algorithms visibly.

Table 3 shows the results obtained by using ALO algorithm and the results are compared with GA [10], PSO [13], SA [15], BBO [16], FFA [17], and MFO [23] algorithm. The table contains the normalized values of current amplitude excitation weights, inter-element spacing, SLL, 3-dB beam width, and the mutual coupling values achieved by using different algorithms for 10 elements CAA design. Table 3 shows that the authors have obtained muchimproved results of SLL and 3-dB beam width by employing ALO algorithm compared to other well-established algorithms. The SLL value for the uniform pattern for 10 elements CAA design is −3.597 dB which is improved to −9.811 dB, −12.307 dB, −13.00 dB, −13.95 dB, −13.30 dB, and −15.81 dB by using GA, PSO, SA, BBO, FFA, and MFO algorithm, respectively. Now by employing ALO algorithm far better results of SLL of −15.91 dB is achieved. The reduction of SLL value is improved to 62.26%, 29.35%, 22.46%, 14.12%, 19.69%, and 0.69% with respect to GA, PSO, SA, BBO, FFA, MFO algorithm as given in Table 3. Similarly, the 3-dB beam width obtained by using GA,

Table 2. Results achieved by employing ALO compared to the other optimization techniques for $N = 8$ elements CAA.

Algorithms	Currents	Distance	SLL (dB)	3-dB beam width (°)	Mutual Coupling	Improvement in SLL reduction (%)
GA [10]	0.328 0.2537 0.7849 1.0000 0.9171 0.5183 0.6176 0.4612	0.1739 0.3144 0.6620 0.7425 0.6297 0.8929 0.4633 0.5267	−9.811	32	0.0118	61.75
PSO [13]	0.7765 0.3928 0.6069 0.8446 1.0000 0.7015 0.9321 0.3583	0.3590 0.5756 0.2494 0.7638 0.6025 0.8311 0.7809 0.3308	−10.799	32	0.0080	46.95
SA [15]	0.3047 0.4840 0.7751 0.9867 0.3371 0.4422 0.4067 0.6807	0.9997 0.7743 0.9042 0.5652 0.8056 0.7818 0.5848 0.4594	−12.00	30.60	0.0193	32.25
BBO [16]	1.0000 0.6736 0.1678 1.0000 0.9088 0.6553 0.7571 1.0000	0.6341 1.0000 1.8892 0.8456 0.5693 1.1639 1.3329 1.6367	−12.24	31.60	0.0203	29.65
FFA [17]	0.8251 0.7018 0.9962 0.9964 0.4933 0.5697 0.4228 0.1669	0.3377 0.8274 0.8575 0.6306 0.8538 0.7092 0.2499 0.1895	−13.00	33.10	0.0040	22.07
MFO [23]	0.2600 0.0018 0.1475 0.3229 0.3356 0.1457 0.2632 0.1956	0.3614 0.5851 0.7795 0.9018 0.5446 0.9026 1.3872 0.3421	−15.78	32.76	0.0149	0.57
ALO	0.6811 0.3620 0.9430 0.9771 0.3365 0.0025 0.7102 0.2550	0.3391 0.7675 0.8498 0.6081 0.8460 0.3281 0.4616 0.3264	−15.87	30.16	0.0146	

https://doi.org/10.1017/S1759078720000914 Published online by Cambridge University Press

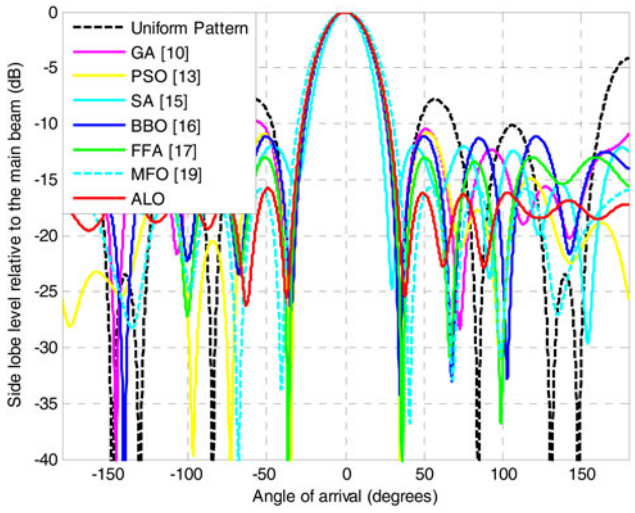


Fig. 4. Array patterns obtained by employing different optimization techniques for the 8-elements CAA design.

PSO, SA, BBO, FFA, and MFO algorithms is 32°, 24.34°, 18.40°, 16.60°, 25.06°, and 30.60°, respectively. However, the authors have obtained a muchimproved value of 16.55°, 3-dB beam width by employing ALO algorithm. The mutual coupling values obtained by using GA, PSO, SA, BBO, FFA, MFO, and ALO algorithms are 0.0094, 0.0063, 0.0154, 0.0115, 0.0092, 0.135, and 0.0153, respectively.

Figure 5 shows the graphical representation of the radiation patterns obtained by using different algorithms for 12 elements of CAA design. The figure also shows the comparison with the uniform pattern obtained by using uniform current excitation to all elements of the array having a half wavelength inter-element spacing. The graphical plots of Fig. 5 show clearly that ALO algorithm-based results yield the lowest SLL and 3-dB beam width values as compared to those of the values achieved by using other well-established algorithms.

Table 4 depicts the comparative results of the non-uniformly excited and non-uniformly spaced 12 elements CAA design using different algorithms. The authors have applied the ALO algorithm for 12 elements CAA design and obtained far better results of SLL and 3-dB beam width compared to the other well-established algorithms. The SLL values obtained by using GA [10], PSO [13], SA [15], BBO [16], FFA [17], and MFO [23] algorithms are −11.83 dB, −13.67 dB, −13.91 dB, −14.37 dB, −14.21 dB, and −17.79 dB, respectively; whereas, the authors have achieved much better results of SLL of −18.02 dB by employing ALO algorithm. The reduction of SLL value is improved to 52.32%, 31.82%, 29.54%, 25.40%, 26.81%, and 1.29% with respect to GA, PSO, SA, BBO, FFA, MFO algorithm as given in Table 4. The 3-dB beam width values obtained by using GA, PSO, SA, BBO, FFA, and MFO algorithms are 20.80°, 21.20°, 19.60°, 19.80°, 20.91°, and 16.92°, respectively; whereas, by employing ALO algorithm far better 3-dB beam width results of 16.86° is achieved. The mutual coupling value achieved by using GA, PSO, SA, BBO, FFA, MFO ALO algorithms is 0.0112, 0.0056, 0.0117, 0.0102, 0.0082, 0.0135, and 0.0131, respectively.

The results of Table 4 are graphically plotted in Fig. 6 which confirms that ALO algorithm yields the lowest SLL and 3-dB beam width values as compared to the other well-established algorithms.

Table 3. Results achieved by employing ALO compared to the other optimization techniques for $N = 10$ elements CAA.

Algorithms	Currents	Distance	SLL (dB)	3-dB beam width (°)	Mutual Coupling	Improvement in SLL reduction (%)
GA [10]	0.9545 0.4283 0.3392 0.9074 0.8086 0.4533 0.5634 0.6015 0.7045 0.5948	0.3641 0.4512 0.2750 1.6373 0.6902 0.9415 0.4657 0.2898 0.6456 0.3282	−9.811	32	0.0094	62.26
PSO [13]	1.0000 0.7529 0.7519 1.0000 0.5062 1.0000 0.7501 0.7524 1.0000 0.5067	0.3170 0.9654 0.3859 0.9654 0.3185 0.3164 0.9657 0.3862 0.9650 0.3174	−12.307	24.34	0.0063	29.35
SA [15]	0.6920 0.5679 0.5937 0.6703 0.9693 0.6014 0.3575 0.3020 0.5908 0.9718	0.6221 0.9880 0.7777 0.9934 0.6217 0.9514 0.7626 0.5980 0.7655 0.9410	−13.00	18.40	0.0154	22.46
BBO [16]	1.0000 1.0000 1.0000 0.3819 0.8970 1.0000 0.7679 0.8899 0.7246 1.0000	0.5301 1.0603 1.3264 1.0000 0.4307 0.4408 1.5276 1.3255 1.0000 0.5904	−13.95	16.60	0.0115	14.12
FFA [17]	0.7081 0.2682 0.3713 0.4100 0.8800 0.9665 0.4165 0.5813 0.7494 0.5403	0.3810 0.7453 0.2668 0.3142 1.0000 0.6032 0.9706 0.5713 0.8800 0.3376	−13.30	25.06	0.0092	19.69
MFO [23]	0.7187 0.1657 0.3774 0.8951 0.2877 0.8744 0.3368 0.2302 0.7062 0.7173	0.3608 0.7597 0.5501 0.9709 0.3057 0.3187 0.9227 0.6595 0.7110 0.3580	−15.81	30.60	0.0135	0.69
ALO	0.3199 0.3449 0.2065 0.5042 0.4938 0.1445 0.2668 0.0449 0.3285 0.4783	0.6802 1.0272 1.8988 1.5758 0.5528 1.1360 1.5078 0.8029 0.8502 0.6073	−15.92	16.55	0.0153	

https://doi.org/10.1017/S1759078720000914 Published online by Cambridge University Press

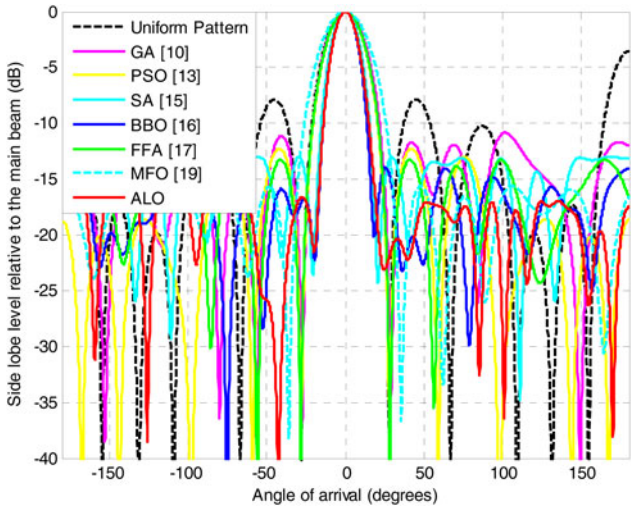


Fig. 5. Array patterns obtained by employing different optimization techniques for the 10-elements CAA design.

The overall inference regarding the numerical results shows that the ALO algorithm-based approach for the design of 8, 10, 12 elements CAA for minimizing the SLL and 3-dB beam width considering the mutual coupling performs exceptionally well. All the simulation results and their graphical plots of far-field radiation patterns reveal the superior optimizing capability of ALO over the other well-established algorithms.

Convergence profile plots of the ALO algorithm

The minimum cost function values against the number of iteration cycles are recorded to get the convergence profile. Figure 7 shows the convergence plots of the ALO algorithm for the design of 8, 10, 12 elements CAA considering the mutual coupling effect.

The above plots of convergence expose the outstanding performance of the ALO algorithm in terms of stability and convergence speed.

Accuracy test of ALO

The statistical parameters of *CF* values obtained by employing the ALO algorithm after 50 independent execution for the synthesis of 8, 10, and 12 elements CAA are given in Table 5.

Table 5 shows that the variation of *CF* values for the ALO algorithm-based design is small enough for the synthesis of 8, 10, and 12 elements CAA design which proves the robustness and stability of the proposed approach.

Box and Whisker plots

The ALO algorithm has been executed for 50 trial runs to achieve the best results and the resulting *CF* values attained in each run have been used for box and whisker plots [25]. Figure 8 shows the box and whisker plots obtained by employing ALO for the 8, 10, and 12 elements CAA design considering the mutual coupling.

Upper and lower ends of the boxes represent the 75th and 25th percentiles, respectively. Median is represented by tringle. The whiskers are the lines extending from each end of the boxes to show the extent of the rest of the data. Outliners are the data with values beyond the end of the whisker. For

Table 4. Results achieved by employing ALO compared to the other optimization techniques for $N = 12$ elements CAA.

Algorithms	Currents	Distance	SLL (dB)	−3 dB beam width (°)	Mutual Coupling	Improvement in SLL reduction (%)
GA [10]	0.2064 0.5416 0.2246 0.6486 0.7212 0.7913 0.5277 0.3495 0.5125 0.4475 0.5233 0.8553	0.4936 0.4184 1.4474 0.7577 0.4204 0.5784 0.4520 0.8872 0.7514 0.4202 0.4223 0.7234	−11.83	20.80	0.0112	52.32
PSO [13]	0.9554 0.6441 0.7109 0.7769 1.0000 1.0000 0.3958 0.7162 0.6746 0.7695 0.9398 0.6145	0.2569 0.8509 0.6607 0.7057 0.8540 0.3734 0.1609 0.8321 0.6464 0.7079 0.8330 0.2682	−13.67	21.20	0.0056	31.82
SA [15]	0.6231 0.3990 0.3418 0.6054 0.9444 0.7380 0.6741 0.3001 0.4311 0.5435 0.4195 0.9795	0.8315 0.7910 0.6699 0.8087 0.7347 0.5331 0.4777 0.8960 0.4874 0.8657 0.3461 0.5105	−13.91	19.60	0.0117	29.54
BBO [16]	1.0000 0.6501 0.6224 0.5020 0.5540 1.0000 0.6683 0.7234 0.4410 0.5123 0.4793 1.000	0.6704 1.0000 1.3046 0.8081 1.0000 0.4031 0.6183 1.1574 1.3465 0.6551 1.0000 0.6539	−14.37	19.80	0.0102	25.40
FFA [17]	0.9175 0.3153 0.5814 0.6311 0.9629 0.9903 0.3297 0.4345 0.6820 0.4397 0.7151 0.7605	0.3171 0.8105 0.5833 0.7609 0.8946 0.4747 0.9868 0.2509 0.2932 0.7748 0.6722 0.3955	−14.21	20.91	0.0082	26.81
MFO [23]	0.1201 0.0903 0.0450 0.0607 0.1104 0.1958 0.1657 0.0710 0.0925 0.0903 0.1401 0.2206	0.5458 1.1054 0.6651 1.3603 1.1902 0.4503 0.4954 1.1005 1.3665 0.7849 1.0405 0.5209	−17.79	16.92	0.0135	1.29
ALO	0.2638 0.3065 0.0010 0.1841 0.4670 0.4791 0.1450 0.0430 0.2104 0.0941 0.2882 0.4630	0.6095 1.0829 0.6974 1.2351 1.5781 0.5559 1.1448 0.5371 0.8700 0.8301 0.9845 0.5070	−18.02	16.86	0.0131	

https://doi.org/10.1017/S1759078720000914 Published online by Cambridge University Press

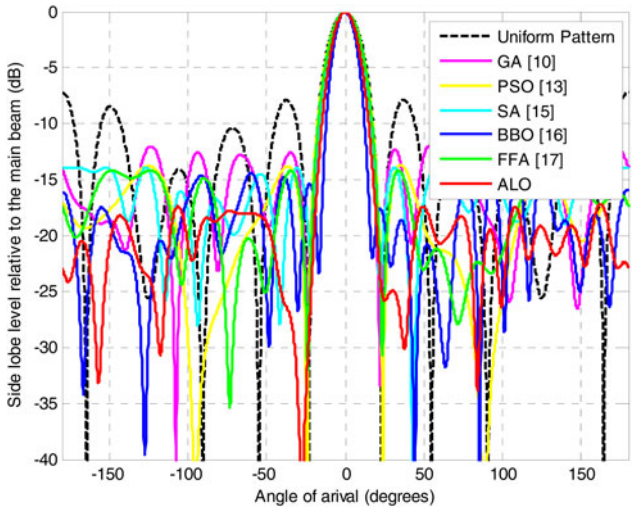


Fig. 6. Array patterns obtained by employing different optimization techniques for the 12-elements CAA design.

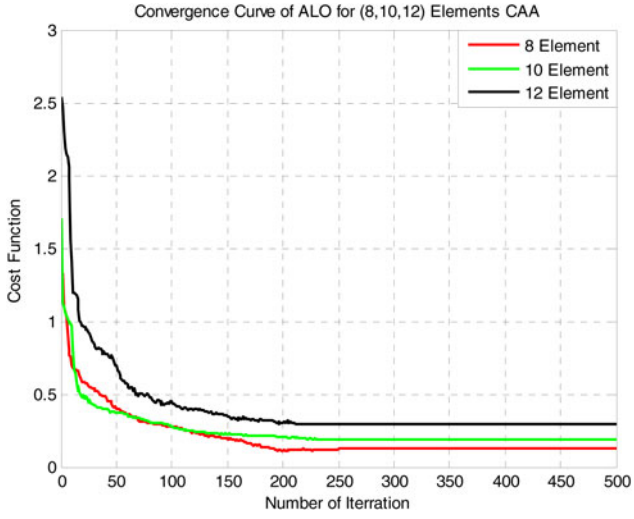


Fig. 7. Convergence plots of 8, 10, and 12 elements CAA considering the mutual coupling effect obtained by employing ALO.

Table 5. Statistical performance of CF values achieved by employing ALO.

No. of Elements	Minimum CF	Maximum CF	Mean CF	Standard deviation of CF
8	0.1255	0.2731	0.2113	0.0311
10	0.1922	0.3764	0.3183	0.0287
12	0.2954	0.5124	0.4331	0.0495

8-elements CAA design, the median value of *CF* is 0.2072, and the range of variation of *CF* value is from 0.1255 to 0.2731. Similarly, for 10-elements and 12-elements CAA design, the median values of the *CF* are 0.2907 and 0.4011, respectively. The range of variations of *CF* for 10 elements and 12 elements CAA design is from 0.1922 to 0.3764 and 0.2954 to 0.5124, respectively.

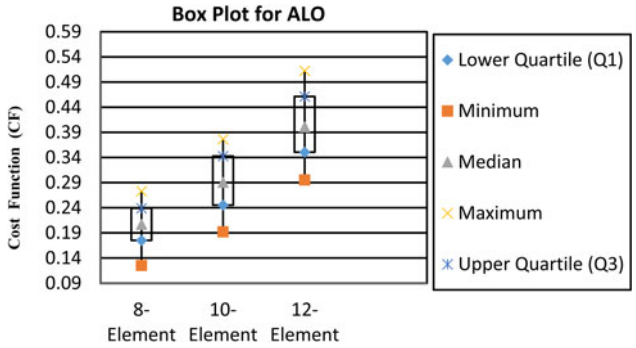


Fig. 8. Box and Whisker plots for ALO-based 8, 10, and 12 elements CAA design considering the mutual coupling.

The range of variations of *CF* values is small for 8, 10, and 12 elements CAA design by employing the ALO algorithm. Thus from the whisker plots, it is evident that the ALO-based design offers robust and stable results.

Conclusion

This paper presents an efficient method of optimal far-field radiation pattern synthesis of a non-uniform single ring circular antenna array considering the mutual coupling effect by employing the evolutionary optimization technique known as ant lion optimization. The mutual coupling is considered in the cost function first time in this paper for the synthesis of non-uniform single ring CAA. The results achieved by employing different algorithms for the synthesis of non-uniform single ring CAA for suppressing the SLL as well as reducing the 3-dB beam width are compared in this paper. The performance analysis of different algorithms for the synthesis of non-uniform single ring CAA shows that the ALO algorithm has an excellent prospect to be used as a proficient optimizer to determine the optimal current amplitude excitation weights and the inter-element distances among the elements of the array for the design and pattern modeling of a non-uniform single ring circular antenna array.

Acknowledgements. The authors express their sincere gratitude to SERB, DST, Govt. of India for funding the project under the grant EEQ/2017/000519 dated 23 March 2018. The authors are also thankful to Visvesvaraya fellowship offered by Meity, Govt. of India.

References

1. **Balanis CA** (1997) *Antenna Theory Analysis and Design*, 2nd Edn. New York: John Willey and Son.
2. **Elliott RS** (2003) *Antenna Theory and Design*, Revised Edn. New Jersey: IEEE Press.
3. **Lui HS, Hui HT and Leong MS** (2009) A note on the mutual-coupling problems in transmitting and receiving antenna arrays. *IEEE Antennas and Propagation Magazine* **51**, 171–176.
4. **Gupta I and Ksienski A** (1983) Effect of mutual coupling on the performance of adaptive arrays. *IEEE Transactions on Antennas and Propagation* **31**, 785–791.
5. **Chakravorty P and Mandal D** (2016) Radiation pattern correction in mutually coupled antenna arrays using parametric assimilation technique. *IEEE Transactions on Antennas and Propagation* **64**, 4092–4095.
6. **Das A, Mandal D, Ghoshal SP and Kar R** (2017) An efficient Side lobe reduction technique considering mutual coupling effect in linear array antenna using BAT algorithm. *Swarm and Evolutionary Computation* **35**, 26–40.

https://doi.org/10.1017/S1759078720000914 Published online by Cambridge University Press

7. **Mandal D, Ghoshal SP and Bhattacharjee AK** (2011) Wide null control of symmetric linear antenna array using novel particle swarm optimization. *International Journal of RF and Microwave Computer-Aided Engineering* **21**, 376–382.
8. **Haupt RL and Werner DH** (2007) Genetic algorithms in electromagnetics. *IEEE Press & Willey-Interscience*.
9. **Haupt RL** (1995) An Introduction to genetic algorithm for electromagnetics. *IEEE Antennas and Propagation Magazine* **37**, 7–15.
10. **Panduro MA, Mendez AL, Dominguez R and Romero G** (2006) Design of non-uniform circular antenna arrays for side lobe reduction using the method of genetic algorithm. *International Journal of Electronics Communication (AEU)* **60**, 713–717.
11. **Kennedy J and Eberhart R** (1995) Particle swarm optimization, *ICNN'95–International Conference on Neural Network*, Perth, WA, Australia, vol. 4, pp. 1942–1948.
12. **Boehringer DW and Werner DH** (2004) Particle swarm optimization versus genetic algorithm for phased array synthesis. *IEEE transaction on Antennas and Propagation* **52**, 771–779.
13. **Sahib M, Najjar Y, Dib N and Khodier M** (2008) Design of non-uniform circular antenna arrays using the particle swarm optimization. *Journal of Electrical Engineering* **59**, 216–220.
14. **Ingber L** (1993) Simulated annealing: practice versus theory. *Mathematical and Computer Modelling* **18**, 29–57.
15. **Rattan M, Patterh MS and Sohi BS** (2009) Optimization of circular antenna arrays of isotropic radiators using simulated annealing. *International Journal of Microwave and Wireless Technologies* **1**, 441–446.
16. **Singh U and Kamal TS** (2011) Design of non-uniform circular antenna arrays using biogeography-based optimization. *IET Microwaves, Antennas and Propagation* **5**, 1365–1370.
17. **Sharaqa A and Dib N** (2013) Circular antenna array synthesis using firefly algorithm. *International Journal of RF and Microwave Computer-Aided Engineering* **24**, 139–146.
18. **Morabito AF, Donato LD and Isernia T** (2018) Orbital angular momentum antennas: understanding actual possibilities through the aperture antennas theory. *IEEE Antennas and Propagation Magazine* **60**, 59–67.
19. **Mirjalili S** (2015) The ant lion optimizer. *Advances in Engineering Software* **83**, 80–98.
20. **Saxena P and Kothari A** (2016) Ant lion optimization algorithm to control side lobe level and null depths in linear antenna arrays. *International Journal of Electronics and Communication (AEU)* **70**, 1339–1349.
21. **Gupta E and Saxena A** (2016) Performance evaluation of antlion optimizer based regulator in automatic generation control of interconnected power system. *Journal of Engineering* **2016**, 4570617.
22. **Tung NS and Chakravorty S** (2016) Ant lion optimizer based approach for optimal scheduling of thermal units for small scale electrical economic power dispatch problem. *International Journal of Grid and Distributed Computing* **9**, 211–224.
23. **Das A, Mandal D, Ghoshal SP and Kar R** (2018) Moth flame optimization-based design of linear and circular antenna array for side lobe reduction. *International Journal of Numerical Modelling-Electronic Networks. Devices and Fields* **32**, 1–15.
24. **Eiben AE and Smit SK** (2011) Parameter tuning for configuring and analyzing evolutionary algorithms. *Swarm and Evolutionary Computation* **1**, 19–31.
25. **De BP, Kar R, Mandal D and Ghoshal SP** (2016) Soft computing-based approach for the optimal design of on-chip comparator and folded-cascode op-amp using colliding bodies optimization. *International Journal of Numerical Modelling Electronic Networks. Devices and Fields* **29**, 873–896.



Avishek Das completed his B.E. degree in Electronics and Communication Engineering and M.Tech. in E.C.E (Microwave) from The University of Burdwan, West Bengal, India in 2008 and 2010, respectively. He received an MBA degree in Human Resource from Sikkim Manipal University in the year 2014 and completed his Ph.D. degree in 2020 from National Institute of Technology, Durgapur, West Bengal, India under Visvesvaraya Ph.D. Scheme for Electronics and IT, Ministry of Electronics and IT, Government of India. Presently, he is working as Assistant Professor in the Department of Electronics and Communication Engineering, Haldia Institute of Technology, Haldia, West Bengal, India and associated as a post Ph.D. researcher at National Institute of Technology, Durgapur, on the project funded by Science and Engineering Research Board, Department of Science and Technology, Government of India (Grant No. EEQ/2017/000519 dated 23/03/2018). His research interests include the application of evolutionary optimization techniques for the design of Antenna Arrays.



Durbadal Mandal passed B. E. degree in Electronics and Communication Engineering, from Regional Engineering College, Durgapur, West Bengal, India in the year 1996. He received the M. Tech. and Ph. D. degrees from National Institute of Technology, Durgapur, West Bengal, India in the year 2008 and 2011 respectively. Presently, he is working in National Institute of Technology, Durgapur, West Bengal, India, as Associate Professor in the Department of Electronics and Communication Engineering. His research interest includes Array Antenna design; filter Optimization via Evolutionary Computing Techniques. He has published more than 350 research papers in International Journals and Conferences.



Rajib Kar passed B. E. degree in Electronics and Communication Engineering, from Regional Engineering College, Durgapur, West Bengal, India in the year 2001. He received the M. Tech. and Ph. D. degrees from National Institute of Technology, Durgapur, West Bengal, India in the year 2008 and 2011, respectively. Presently, he is working in National Institute of Technology, Durgapur, West Bengal, India, as Associate Professor in the Department of Electronics and Communication Engineering. His research interest includes VLSI circuit optimization, Signal Processing using Evolutionary Computing Techniques. He has published more than 350 research papers in International Journals and Conferences.

https://doi.org/10.1017/S1759078720000914 Published online by Cambridge University Press